



1 **Impact of dust addition on the microbial food web under present and future**  
2 **conditions of pH and temperature**

3

4 Julie Dinasquet<sup>1,2\*</sup>, Estelle Bigeard<sup>3</sup>, Frédéric Gazeau<sup>4</sup>, Farooq Azam<sup>1</sup>, Cécile Guieu<sup>4</sup>, Emilio  
5 Marañón<sup>5</sup>, Céline Ridame<sup>6</sup>, France Van Wambeke<sup>7</sup>, Ingrid Obernosterer<sup>2</sup> and Anne-Claire  
6 Baudoux<sup>3</sup>

7 <sup>1</sup> Marine Biology Research Division, Scripps Institution of Oceanography, UCSD, USA

8 <sup>2</sup> Sorbonne Université, CNRS, Laboratoire d'Océanographie Microbienne, LOMIC, France

9 <sup>3</sup> Sorbonne Université, CNRS, Station Biologique de Roscoff, UMR 7144 Adaptation et  
10 Diversité en Milieu Marin, France

11 <sup>4</sup> Sorbonne Université, CNRS, Laboratoire d'Océanographie de Villefranche, LOV, 06230  
12 Villefranche-sur-Mer, France

13 <sup>5</sup> Department of Ecology and Animal Biology, Universidade de Vigo, Spain

14 <sup>6</sup> CNRS-INSU/IRD/MNHN/UPMC, LOCEAN: Laboratoire d'Océanographie et du Climat:  
15 Expérimentation et Approches Numériques, UMR 7159

16 <sup>7</sup> Aix-Marseille Université, CNRS/INSU, Université de Toulon, IRD, Mediterranean Institute of  
17 Oceanography, UM110, France

18 \*Corresponding: [jdinasquet@ucsd.edu](mailto:jdinasquet@ucsd.edu), present address: Center for Aerosol Impact on Chemistry  
19 of the Environment (CAICE), Scripps Institution of Oceanography, UCSD, USA

20 **Keywords:** bacteria, microeukaryotes, virus, community composition, top-down



## 21 **Abstract**

22 In the oligotrophic waters of the Mediterranean Sea, during the stratification period, the  
23 microbial loop relies on pulsed inputs of nutrients through atmospheric deposition of aerosols  
24 from both natural (Saharan dust) and anthropogenic origins. While the influence of dust  
25 deposition on microbial processes and community composition is still not fully constrained, the  
26 extent to which future environmental conditions will affect dust inputs and the microbial  
27 response is not known. The impact of atmospheric wet dust deposition was studied both under  
28 present and future (warming and acidification) environmental conditions through experiments in  
29 300 L climate reactors. Three dust addition experiments were performed with surface seawater  
30 collected from the Tyrrhenian Sea, Ionian Sea and Algerian basin in the Western Mediterranean  
31 Sea during the PEACETIME cruise in May-June 2017. Top-down controls on bacteria, viral  
32 processes and community, as well as microbial community structure (16S and 18S rDNA  
33 amplicon sequencing) were followed over the 3-4 days experiments. Different microbial and  
34 viral responses to dust were observed rapidly after addition and were most of the time higher  
35 when combined to future environmental conditions. The input of nutrients and trace metals  
36 changed the microbial ecosystem from bottom-up limited to a top-down controlled bacterial  
37 community, likely from grazing and induced lysogeny. The composition of mixotrophic  
38 microeukaryotes and phototrophic prokaryotes was also altered. Overall, these results suggest  
39 that the effect of dust deposition on the microbial loop is dependent on the initial microbial  
40 assemblage and metabolic state of the tested water, and that predicted warming, and acidification  
41 will intensify these responses, affecting food web processes and biogeochemical cycles.



## 42        **1. Introduction**

43        Input of essential nutrients and trace metals through aerosol deposition is crucial to the ocean  
44        surface water biogeochemistry and productivity (at the global scale: *e.g.*, Mahowald et al., 2017;  
45        in the Mediterranean Sea: *e.g.*, Guieu and Ridame, 2020) with episodic fertilization events  
46        driving microbial processes in oligotrophic regions such as the Pacific Ocean, the Southern  
47        Ocean and the Mediterranean Sea.

48        The summer Mediterranean food web is characterized by low primary production (PP) and  
49        heterotrophic prokaryotic production (more classically abbreviated as BP for bacterial  
50        production) constrained by nutrient availability further limiting dissolved organic matter (DOM)  
51        utilization and export, resulting in DOM accumulation. Therefore, inputs of bioavailable  
52        nutrients through deposition of atmospheric particles are essential to this microbial ecosystem.  
53        Indeed, these nutrient pulses have been shown to support microbial processes but the degree to  
54        which the microbial food web is affected might be dependent on the degree of oligotrophy of the  
55        water (Marín-Beltrán et al., 2019; Marañón et al., 2010).

56        In the Mediterranean Sea, dust deposition stimulates PP and N<sub>2</sub> fixation (Guieu et al., 2014;  
57        Ridame et al., 2011) but also BP, bacterial respiration, virus production, grazing activities, and  
58        can alter the composition of the microbial community (*e.g.*, Pulido-Villena et al., 2014; Tsiola et  
59        al., 2017; Guo et al., 2016; Pitta et al., 2017; Marín-Beltrán et al., 2019). Overall, in such  
60        oligotrophic system, dust deposition appears to predominantly promote heterotrophic activity  
61        which will increase respiration rates and CO<sub>2</sub> release.

62        Anthropogenic CO<sub>2</sub> emissions are projected to induce an increase in seawater temperature  
63        and an accumulation of CO<sub>2</sub> in the ocean, leading to its acidification and an alteration of ocean  
64        carbonate chemistry (IPCC, 2014). In response to ocean warming and increased stratification,



65 low nutrient low chlorophyll (LNLC) regions such as the Mediterranean Sea, are projected to  
66 expand in the future (Durrieu de Madron et al., 2011). Moreover, dust deposition is also expected  
67 to increase due to desertification (Moulin and Chiapello, 2006). Hence, in the future ocean, the  
68 microbial food web might become even more dependent on atmospheric deposition of nutrients.  
69 Expected increased temperature and acidification might have complex effects on the microbial  
70 loop by modifying microbial and viral and community (*e.g.*, Highfield et al., 2017; Krause et al.,  
71 2012; Hu et al., 2021; Allen et al., 2020; Malits et al., 2021). While increasing temperature in  
72 combination with nutrient input might enhance heterotrophic bacterial growth (Degerman et al.,  
73 2012; Morán et al., 2020) more than PP (Marañón et al., 2018), future environmental conditions  
74 could push even further this microbial community towards heterotrophy. But so far, the role of  
75 dust on the microbial food web in future climate scenarios is unknown.

76 Here, we studied the response of Mediterranean microbial and viral communities (*i.e.*, viral  
77 strategies, microbial growth, and controls, as well as community composition) to simulated wet  
78 Saharan dust deposition during onboard minicosm experiments conducted in three different  
79 basins of the Western and Central Mediterranean Sea under present and future projected  
80 conditions of temperature and pH. To our knowledge, this is the first study assessing the effect of  
81 atmospheric deposition on the microbial food web under future environmental conditions.



## 82        2. Material & Method

### 83        *2.1 Experimental set-up*

84            During the ProcEss studies at the Air-sEa Interface after dust deposition in the  
85        Mediterranean sea project cruise (PEACETIME), onboard the R/V “Pourquoi Pas ?” in  
86        May/June 2017, three experiments were conducted in 300 L climate reactors (minicosms) filled  
87        with surface seawater collected at three different stations (Table 1), in the Tyrrhenian Sea (TYR),  
88        Ionian Sea (ION) and in the Algerian basin (FAST). The experimental set-up is described in  
89        details in Gazeau et al. (2020). Briefly, the experiments were conducted for 3 days (TYR and  
90        ION) and 4 days (FAST) in trace metal free conditions, under light, temperature and pH-  
91        controlled conditions following ambient or future projected conditions of temperature and pH.  
92        For each experiment, the biogeochemical evolution of the water, after dust deposition, under  
93        present and future environmental conditions was followed in three duplicate treatments: i)  
94        CONTROL (C1, C2) with no dust addition and under present pH and temperature conditions, ii)  
95        DUST (D1, D2) with dust addition under present environmental conditions and iii)  
96        GREENHOUSE (G1, G2) with dust addition under projected temperature and pH for 2100  
97        (IPCC, 2014; ca. +3 °C and -0.3 pH units). The same dust analog was used as during the DUNE  
98        2009 experiments described in Desboeufs et al. (2014) and the same dust wet flux of 10 g m<sup>-2</sup>  
99        was simulated. Such deposition event represents a high but realistic scenario, as several studies  
100        reported even higher short deposition events in this area of the Mediterranean Sea (Ternon et al.,  
101        2010; Bonnet and Guieu, 2006; Loÿe-Pilot and Martin, 1996). After mixing the dust analog (3.6  
102        g) in 2 L of ultrahigh-purity water, this solution was sprayed at the surface of the dust amended  
103        treatments (D1, D2 and G1, G2; Gazeau et al., 2020).



104 Samples were taken at t-12h (while filling the tanks), t0 (just before dust addition), t1h,  
105 t6h, t12h, t24h, t48h, t72h and t96h (after dust addition, and t96h only for FAST).

### 106 2.2. Growth rates, mortality, and top down controls

107 BP was estimated at all sampling points from rates of  $^3\text{H}$ -Leucine incorporation  
108 (Kirchman et al., 1985; Smith and Azam, 1992) as described in Gazeau et al. (2021). Briefly,  
109 triplicate 1.5 mL samples and one blank were incubated in the dark for 1-2 h in two temperature-  
110 controlled incubators maintained respectively at ambient temperature for C1, C2, D1 and D2 and  
111 at ambient temperature +3 °C for G1 and G2. HB, *Synechococcus*, picoeukaryotes and  
112 heterotrophic nanoflagellates (HNF) abundances were measured by flow cytometry as described  
113 in Gazeau et al. (2020). Bacterial cell specific growth rates were estimated assuming exponential  
114 growth and a carbon to cell ration of 20 fg C cell<sup>-1</sup> (Lee and Fuhrman, 1987). Net growth rates  
115 (h<sup>-1</sup>) were calculated from the exponential phase of growth of BP, abundances of *Synechococcus*  
116 and picoeukaryotes cells, observable from at least three successive sampling points. Mortality  
117 was estimated as the difference between HB present between two successive sampling points and  
118 those produced during that time.

### 119 2.3. Viral abundance, production and life strategy

120 Virus abundances were determined on glutaraldehyde fixed samples (0.5% final  
121 concentration, Grade II, Sigma Aldrich, St Louis, MO, USA) stored at -80 °C until analysis. Flow  
122 cytometry analysis was performed as described by Brussaard (2004). Briefly, samples were  
123 thawed at 37 °C, diluted in 0.2 µm filtered autoclaved TE buffer (10:1 Tris-EDTA, pH 8) and  
124 stained with SYBR-Green I (0.5 × 10<sup>-4</sup> of the commercial stock, Life Technologies, Saint-Aubin,  
125 France) for 10 min at 80 °C. Virus particles were discriminated based on their green fluorescence



126 and SSC during 1 min analyses (Fig. S1). All cytogram analyses were performed with the Flowing  
127 Software freeware (Turku Center of Biotechnology, Finland).

128 Viral production and bacterial losses due to phages were assessed by the virus reduction approach  
129 (Weinbauer et al., 2010) at t<sub>0</sub>, t<sub>24</sub> h and t<sub>48</sub>h in all six minicosms. Briefly, 3 L of seawater were-  
130 filtered through 1.2- $\mu$ m-pore-size polycarbonate filter (Whatman©), and heterotrophic  
131 prokaryotes (HB, filtrate) were concentrated by ultrafiltration (0.22  $\mu$ m pore size, Vivaflow 200©  
132 polyethersulfone, PES) down to a volume of 50 mL. Virus-free water was obtained by filtering 1  
133 L of seawater through a 30 kDa pore-size cartridge (Vivaflow 200©, PES). Six mixtures of HB  
134 concentrate (2 mL) diluted in virus-free water (23 mL) were prepared and distributed into 50 mL  
135 Falcon tubes. Three of the tubes were incubated as controls, while the other three were inoculated  
136 with mitomycin C (Sigma-Aldrich, 1  $\mu$ g mL<sup>-1</sup> final concentration) as inducing agent of the lytic  
137 cycle in lysogenic bacteria. All tubes were incubated in darkness in two temperature-controlled  
138 incubators maintained respectively at ambient temperature for C1, C2, D1 and D2 and at ambient  
139 temperature +3 °C for G1 and G2. Samples for HB and viral abundances were collected every 6 h  
140 for a total incubation period of 18 h.

141 The estimation of virus-mediated mortality of HB was performed according to Weinbauer et al.  
142 (2002) and Winter et al. (2004). Briefly, increase in virus abundance in the control tubes represents  
143 lytic viral production (VPL), and an increase in mitomycin C treatments represents total (VPT),  
144 *i.e.*, lytic plus lysogenic, viral production. The difference between VPT and VPL represents  
145 lysogenic production (VPLG). The frequency of lytically infected cells (FLIC) and the frequency  
146 of lysogenic cells (FLC) were calculated as:

$$147 \quad \text{FLIC} = 100 \times \text{VPL} / \text{BS} \times \text{HB}_i \quad (1)$$

$$148 \quad \text{FLC} = 100 \times \text{VPLG} / \text{BS} \times \text{HB}_i \quad (2)$$



149 where  $HB_i$  is the initial HB abundance in the viral production experiment and BS is a theoretical  
150 burst size of 20 viruses per infected cell (averaged BS in marine oligotrophic waters, Parada et al.,  
151 2006).

152

#### 153 2.4 DNA sampling, sequencing and sequence analysis

154 To study the temporal dynamics of the microbial diversity, water samples (3 L) were  
155 collected in acid-washed containers from each minicosm at  $t_0$ ,  $t_{24h}$ , and at the end of the  
156 experiments ( $t_{72h}$  at TYR and ION and  $t_{96h}$  at FAST). Samples were filtered onto 0.2  $\mu\text{m}$  PES  
157 filters (Sterivex©) and stored at  $-80^\circ\text{C}$  until DNA extraction. Nucleic acids were extracted from  
158 the filters using a phenol-chloroform method and DNA was then purified using filter columns from  
159 NucleoSpin® PlantII kit (Macherey-Nagel©) following a modified protocol. DNA extracts were  
160 quantified and normalized at  $5\text{ng } \mu\text{L}^{-1}$  and used as templates for PCR amplification of the V4  
161 region of the 18S rRNA ( $\sim 380$  bp) using the primers TAREuk454FWD1 and TAREukREV3  
162 (Stoeck et al., 2010) and the V4-V5 region of the 16S rRNA ( $\sim 411$  bp) using the primers 515F-Y  
163 ( $5'\text{-GTGYCAGCMGCCGCGGTAA}$ ) and 926R-R ( $5'\text{-CCGYCAATTYMTTTRAGTTT}$ ) (Parada  
164 et al., 2016). Following polymerase chain reactions, DNA amplicons were purified, quantified and  
165 sent to Genotoul (<https://www.genotoul.fr/>, Toulouse, France) for high throughput sequencing  
166 using paired-end 2x250bp Illumina MiSeq. Note that although we used universal primer, Archaea  
167 were mostly not detected and the prokaryotic heterotrophic communities corresponded essentially  
168 to Eubacteria, therefore the taxonomic description referred to the general term ‘bacterial  
169 communities’

170 All reads were processed using the Quantitative Insight Into Microbial Ecology 2 pipeline  
171 (QIIME2 v2020.2, Bolyen et al., 2019). Reads were truncated 350bp based on sequencing





172 quality, denoised, merged and chimera-checked using DADA2 (Callahan et al., 2016). A total of  
173 714 and 3070 amplicon sequence variants (ASVs) were obtained for 16S and 18S respectively.  
174 Taxonomy assignments were made against the database SILVA 132 (Quast et al., 2013) for 16S  
175 and PR2 (Guillou et al., 2013) for 18S. All sequences associated with this study have been  
176 deposited under the BioProject ID: PRJNA693966.

### 177 2.5 Statistics

178 Alpha and beta-diversity indices for community composition were estimated after  
179 randomized subsampling to 26000 reads for 16S rDNA and 19000 reads for 18S rDNA. Analysis  
180 were run in QIIME 2 and in Primer v.6 software package (Clarke and Warwick, 2001).  
181 Differences between the samples richness and diversity were assessed using Kruskal-Wallis  
182 pairwise test. Beta diversity were run on Bray Curtis dissimilarity. Differences between samples'  
183 beta diversity were tested using PERMANOVA (Permutational Multivariate Analysis of  
184 Variance) with pairwise test and 999 permutations. The sequences contributing most to the  
185 dissimilarity between clusters were identified using SIMPER (similarity percentage). A linear  
186 mixed model was performed using the R software (R Core Team, 2020) using the nlme package  
187 (Pinheiro et al., 2014) to test if the amended treatments differed from the controls at t24h and  
188 t72h or t96h.



### 189      3. Results

#### 190      3.1. Microbial growth, mortality and top-down controls

191            Significant increases in heterotrophic bacterial cell specific growth rates were observed in  
192 all experiments with dust under D and G (Fig. 1,  $p \leq 0.016$  after 24 h and 72 h) relative to C, the  
193 highest growth rates relative to C were observed already 24 h after dust seeding. Bacterial net  
194 growth rates were also higher in D and especially in G relative to C (Table 2). *Synechococcus*  
195 and picoeukaryotes net growth rates showed a similar trend (Table 2). Heterotrophic bacterial  
196 mortality was also higher than in C especially at TYR and in G at ION and FAST (Fig. 1). Over  
197 the course of the three experiments, the slope of the linear regression between bacterial biomass  
198 and bacterial production was below 0.4 in the three treatments suggesting a weak bottom up  
199 control (Fig. 2A; Ducklow, 1992). The slope decreased in D and G relative to C. Overall, the top  
200 down index, as described by Morán et al. (2017), was higher in G (0.92) relative to C and D  
201 (0.80). The relationship between log transformed HNF and bacterial abundance (Fig. 3B), plotted  
202 according to the model in Gasol (1994), showed that HNF were below the MRA (Mean realized  
203 HNF abundance) in all treatments, suggesting a top down control of HNF abundance. HNF and  
204 bacteria were weakly coupled in all treatments. The relationship between total viruses and  
205 bacterial abundance was weaker in D and G relative to C (Fig. S2).

206

#### 207      3.2. Viral dynamics and processes

208            The abundance and production of virus-like particles (VLP) increased following an east  
209 to west gradient (Table 1). Viral strategy (lysogenic vs. lytic replication) was also different  
210 between stations, with a higher frequency of lysogenic cells (FLC) at TYR and ION (23 and



211 19%, respectively Table 1) and a higher frequency of lytically infected cells (FLIC) at FAST  
212 (43%, Table 1).

213 During TYR and ION experiments, the relative contribution of VLP populations was similar  
214 and stable over time with Low DNA viruses representing over 80% of the community (Figs. 3  
215 and S3). The Low DNA VLP abundance was however slightly higher in D and G relative to C  
216 after 24 h at TYR and significantly higher at ION after 48h ( $p = 0.037$ ; Fig. S3). In contrast to  
217 the other two stations, at FAST, Giruses were also present and increased in all treatments but  
218 especially in G where they made up to 9% of the viral community at the end of the experiment  
219 (Figs. 3 and S3). The abundance of high DNA viruses at FAST also increased independent of  
220 treatments and accounted for 16 – 18% of the community at the end of the experiment (Figs. 3  
221 and S3).

222 The sampling strategy for production and life strategies of HB viruses allowed to  
223 discriminate independently the effect of i) greenhouse conditions (sampling at T0 before dust  
224 addition), ii) dust addition (sampling at T24) and the combined effects of dust addition and  
225 greenhouse. Lytic viral production (VPL) increased significantly at T0 in G at TYR and ION  
226 compared to C ( $p \leq 0.036$ ). The addition of dust induced higher VPL in D at TYR compared to C  
227 (Fig.1). No significant impact of dust on VPL was observed in G compared to D after 24h for  
228 any of the experiments. Changes in viral infection strategy were observed with G conditions at  
229 T0 where, FLC decreased relative to the non-G treatments at TYR and ION, and especially at  
230 FAST ( $p = 0.047$ ). FLIC increased slightly in G at TYR and ION already at T0. Dust addition  
231 had no detectable significant effect on this parameter for any experiments. Looking at the  
232 relative share between lytic and lysogenic infection, dust addition favored lytic infection at TYR  
233 (no lysogenic bacteria were observed after 24h) but the contribution of both infection strategies



234 remained unchanged compared to C at ION and FAST. Greenhouse conditions also favored  
235 replication through lytic cycle already at T0 for all three experiments and this trend was not  
236 impacted by dust addition.

### 237 3.3. Microbial community composition

238 Microbial community structure, bacteria and micro-eukaryotes from 16S rDNA and 18S  
239 rDNA sequencing respectively, responded to dust addition in all three experiments relative to C  
240 (Figs. 4 and 5). After quality controls, reads were assigned to 714 and 1443 ASVs for 16S and  
241 18S respectively.

#### 242 3.3.1. Bacterial community composition

243 The initial community composition (t-12h) was significantly different at the three stations  
244 (PERMANOVA;  $p = 0.001$ , Fig. S4a, S5). Rapid and significant changes in the bacterial  
245 community composition were observed already 24 h after dust addition (Fig. 4). Despite the  
246 initial different communities, the three stations appeared to converge towards a closer  
247 community composition in response to dust addition (Fig. S5). At TYR, communities in D and G  
248 significantly changed 24 h after dust addition (PERMANOVA;  $p = 0.001$ ). This cluster presented  
249 no significant differences between treatments (D and G) or time (24 and 72 h). The differences  
250 between C and D/G were attributed to a relative increase of ASVs related to different  
251 *Alteromonas* sp., OM60 and *Pseudophaeobacter* sp. and *Erythrobacter* sp.; contribution of  
252 ASVs related to SAR11 and Verrucomicrobia and *Synechococcus* decreased (Table S1a). At  
253 ION, the bacterial community composition significantly changed 24 h after dust addition  
254 (PERMANOVA;  $p = 0.001$ ) and was significantly different between D and G (PERMANOVA;  $p$   
255  $= 0.032$ ). As observed at TYR, no further change occurred between 24 h and the end of the



256 experiment (72 h; Fig. 4). The difference between the controls and dust amended minicosms  
257 were assigned to an increase of ASVs related to different *Alteromonas* sp., *Erythrobacter* sp.,  
258 *Dokdonia* sp. and OM60, and a decrease of ASVs related to SAR11, *Synechococcus*,  
259 Verrucomicrobia, Rhodospirillales and some Flavobacteria (Table S1b). Several ASVs related to  
260 *Alteromonas* sp., *Synechococcus* sp. and *Erythrobacter* sp. were further enriched in G compared  
261 D while *Dokdonia* sp. was mainly present in D. At FAST, the bacterial community after 24 h  
262 only significantly changed in G (PERMANOVA;  $p = 0.011$ ; Fig. 4). However, after 96 h, the  
263 community in D and G were similar and appeared to transition back to the initial state at 96 h  
264 (PERMANOVA;  $p = 0.077$ ). The higher relative abundance in *Erythrobacter* sp., *Synechococcus*  
265 sp., different ASVs related to *Alteromonas* sp. and Flavobacteria appeared to contribute mainly  
266 to the difference between C and D/G (Table S1) while ASVs related to SAR11,  
267 Verrucomicrobia, *Celeribacter* sp. *Thalassobius* sp. and Rhodospirillales were mainly present in  
268 C (Table S1c).

### 269 3.3.2 Nano- and micro-eukaryotes community composition

270 The diversity of initial community was large (Fig. S5) and significantly different at the three  
271 stations (PERMANOVA;  $p = 0.001$ ; Fig. S4b). At TYR, the nano- and micro-eukaryotes  
272 community responded rapidly (24 h) to dust addition (PERMANOVA;  $p = 0.003$ ). This initial  
273 high diversity disappeared after 72 h, with similar communities in all minicosms (Fig. S5). They  
274 were significantly different from initial and t24h communities ( $p = 0.002$  and  $0.03$  respectively;  
275 Fig 5) in D/G. The variations at t24h were attributed to changes in the dinoflagellate  
276 communities in particular to an increase in ASVs related to *Heterocapsa rotundata*,  
277 Gymnodiniales and Gonyaulacales as well as to an increase in Chlorophyta (Table S2a). At ION,  
278 no significant changes were observed between C and D/G after 24 h. However, after 72 h, the



279 communities were significantly different in D ( $p = 0.018$ ) and G ( $p = 0.05$ ) compared to the  
280 communities at t24h in these treatments (Table S2B). In D, diversity was significantly higher at  
281 t72h compared to t24h and to C at the same sampling time ( $p = 0.036$ ). In contrast, diversity in G  
282 at t72h was lower than at t24h and lower to the one observed in C at the same sampling time ( $p =$   
283  $0.066$ ; Fig S6). These differences were mainly attributed to changes in ASVs related to  
284 dinoflagellates and to the increase at t72h of *Emiliana huxleyi* and Chlorophyta in D and G,  
285 respectively (Table S2b). At FAST, significant differences were observed between the controls  
286 and initial communities compared to the dust amended (D and G) treatments at t24h ( $p = 0.036$ ).  
287 No major differences were observed between D/G at t24h and t96h ( $p = 0.06$ ). The differences  
288 were mainly attributed to changes in dinoflagellates ASVs and to an increase in Acantharea and  
289 *Emiliana huxleyi* in D and G treatments at t96h (Table S2c).



290        **4. Discussion**

291        Pulsed inputs of essential nutrients and trace metals through aerosol deposition are crucial to  
292 surface microbial communities in LNLC regions such as the Mediterranean Sea (reviewed in  
293 Guieu and Ridame, 2020). Here we assessed the impact of dust deposition on the late spring  
294 microbial loop under present and future environmental conditions on the surface water of three  
295 different Mediterranean basins (Tyrrhenian, TYR; Ionian, ION; and Algerian, FAST). The initial  
296 conditions at the three sampled stations for the onboard experiments are described in more  
297 details in Gazeau et al. (2020). Briefly, very low levels of dissolved inorganic nutrients were  
298 measured at all three stations, highlighting the oligotrophic status of the waters, typical of the  
299 stratified conditions observed in the Mediterranean Sea in late spring/early summer (*e.g.*, Bosc et  
300 al., 2004; D'Ortenzio et al., 2005). Despite similar total chl. *a* concentrations at the three stations  
301 (Gazeau et al., 2020), PP was higher at FAST (Table 1, Gazeau et al., 2021; Marañón et al.,  
302 2021). The initial microbial communities differed substantially between the three stations as  
303 shown by pigments (Gazeau et al., 2020), 18S and 16S rDNA sequencing (this study). DOC  
304 concentrations were slightly higher at TYR where PP was the lowest (Gazeau et al., 2021). HB,  
305 HNF abundances (Gazeau et al., 2020), as well as viral abundance and production increased  
306 following the east to west gradient of the initial water conditions.

307        The dust addition induced similar nitrate + nitrite (NO<sub>x</sub>) and dissolved inorganic phosphate  
308 (DIP) release during all three experiments. Rapid changes were observed on plankton stocks and  
309 metabolisms, suggesting that the impact of dust deposition is constrained by the initial  
310 composition and metabolic state of the investigated community (Gazeau et al., 2020; 2021).  
311 While no direct effect of warming and acidification was observed on the amount of nutrient  
312 released from dust, Gazeau et al., (2020, 2021) showed that biological processes were generally



313 enhanced by these conditions and suggested that deposition may weaken the biological pump in  
314 future climate conditions. Here we are further investigating how dust addition in present and  
315 future conditions affected, on a short-term scale ( $\leq 4$  days), the microbial trophic interactions and  
316 community composition.

#### 317 4.1. Trophic interactions after dust addition under present and future conditions

318 Parallel nutrient enrichment incubations conducted in darkness showed that *in situ*  
319 heterotrophic bacterioplankton communities, were N, P co-limited at TYR, mainly P limited at  
320 ION and N limited at FAST (Van Wambeke et al., 2020). However, the HB appeared to be  
321 weakly bottom up controlled (Ducklow, 1992) in our experiment especially in D and G (Fig 2a).  
322 Such top-down control on the bacterioplankton has been previously observed in the  
323 Mediterranean Sea (Siokou-Frangou et al., 2010) and might increase under future conditions as  
324 suggested by the higher top-down index in G ( $G = 0.92$  vs.  $C/D = 0.80$ , Morán et al., 2017).

325 Bacterial mortality increased relative to controls in D and G at TYR, and only in G at ION  
326 and FAST. The weak coupling between bacteria and viruses, as well as the increased virus  
327 production and relative abundance of lytic cells (see below), only explained a small fraction of  
328 the estimated bacterial mortality (max. 17%), suggesting an additional grazing pressure on  
329 bacteria. HNF abundances increased in D at TYR and at all stations in G (Gazeau et al., 2020),  
330 which could explain the increased bacterial mortality. Increased grazing rate by HNF on bacteria  
331 with dust addition has been previously reported in the Eastern Mediterranean Sea (Tsiola et al.,  
332 2017). While our results suggest a strong grazing pressure on bacteria, HNF appeared to be top-  
333 down controlled as well (Gasol, 1994, Fig 3b), potentially by the increasing populations of  
334 mixotrophic dinoflagellates or Giruses (see below). It is also possible that HB were grazed by





335 mixotrophic nanoflagellates or by larger protozoans, or that the HNF abundance was  
336 underestimated by flow cytometry.

337       Considering the seasonal impact of grazing and viral mortality in the Mediterranean Sea,  
338 where higher grazing pressure and lysogeny were observed in the stratified nutrient-limited  
339 waters in summer (Sánchez et al., 2020), it will be important to further study the seasonal impact  
340 of dust deposition on trophic interactions and indirect cascading impact on microbial dynamics  
341 and community composition.

342

343 *4.2. Viral processes and community during dust enrichment in present and future conditions*

344       Viruses represent pivotal components of the marine food web, influencing genome evolution,  
345 community dynamics, and ecosystem biogeochemistry (Suttle, 2007). The environmental and  
346 evolutionary implications of viral infection differ depending on whether viruses establish lytic or  
347 lysogenic infections. Lytic infections produce virion progeny and result in cell destruction while  
348 viruses undergoing lysogenic infections can replicate as “dormant” prophages without producing  
349 virions or can switch to a lytic productive cycle upon an induction event. Understanding how  
350 viral processes are impacted by changes in environmental conditions, is thus crucial to better  
351 constrain microbial mortality and cascading impacts on marine ecosystems. Aerosol deposition  
352 was already identified as a factor that stimulates virus production and viral induced mortality of  
353 bacteria in the Mediterranean Sea (Pulido-Villena et al., 2014; Tsiola et al., 2017) while the  
354 impact of future environmental conditions remains more controversial (Larsen et al., 2008;  
355 Brussaard et al., 2013; Maat et al., 2014; Vaqué et al., 2019; Malits et al., 2021). The combined



356 effect of aerosol deposition and future conditions of temperature and pH on the viral  
357 compartment has, to our knowledge, never been investigated.

358 The rapid changes in viral production and lifestyle observed in all three experiments support the  
359 idea that the viral component is sensitive to the environmental variability even on short (hourly)-  
360 time scales. The dynamics in viral activities was however impacted differently depending on the  
361 treatments and the experiments. Viral production increased in D and G at TYR and only in G at  
362 ION and FAST. Regarding the G treatments, increase in viral production was detected before  
363 dust addition for all three experiments and remained mostly unchanged for the remaining of the  
364 incubation. This suggests that water warming, and acidification were responsible for most  
365 changes in viral activities while dusts had no detectable impact in such conditions regardless of  
366 the studied station. Based on our results, the most likely explanation for observed changes in  
367 viral production is an activation of a lysogenic to lytic switch. The factors that result in prophage  
368 induction are still not well constrained, but nutrients pulses and elevated temperatures have been  
369 identified as potential stressors (Danovaro et al., 2011 and references therein). Consistent with  
370 the observation of N, P co-limited bacterial community at TYR, it is likely that nutrients released  
371 from dust upon deposition to surface water activate the productive cycle of temperate viruses at  
372 this station. Such mechanism was also speculated during another dust addition study (Pulido-  
373 Villena et al., 2014). Under future conditions (G), the low proportion of lysogens was associated  
374 to higher frequency of lytically infected cells relative to C and D at TYR and ION. These trends  
375 probably reflect an indirect effect of enhanced bacterial growth with increased temperature not  
376 only on prophage induction (Danovaro et al., 2011; Vaqué et al., 2019; Mojica and Brussaard,  
377 2014) but also on the kinetics of lytic infections. Intriguingly, the enhanced viral production did  
378 not translate into marked changes in viral abundance. The abundance of Low DNA virus



379 population, which typically comprises virus of bacteria, actually decreased between t0 and t48h  
380 pointing to possible viral decay, potentially related to an adsorption onto dust particles  
381 (Weinbauer et al., 2009; Yamada et al., 2020) and the potential export of viral particle to deeper  
382 water layers (Van Wambeke et al. 2020). While recurrent patterns emerged from this study, the  
383 amplitude of viral responses varied between the experiments. At TYR, where heterotrophic  
384 metabolism was higher, the dust addition induced higher viral production relative to controls  
385 than at the two other sites, which suggests that viral processes, as other microbial processes, are  
386 dependent on the initial metabolic status of the water.

387 Overall, no marked changes were observed for viral communities and abundances after dust  
388 addition, both under present and future conditions relative to controls, except at FAST where the  
389 abundance of Girus population increased significantly in G from t24h until the end of the  
390 experiment. Giruses typically comprise large double stranded DNA viruses that infect  
391 nanoeukaryotes including photosynthetic (microalgae) and heterotrophic (HNF, amoeba,  
392 choanoflagellate) organisms (Brussaard and Martinez, 2008; Needham et al., 2019; Fischer et al.,  
393 2010; Martínez et al., 2014). The presence of Giruses at FAST in this treatment might be  
394 explained by the increase in nano-eukaryote abundances at t72h and their decline after 96 h of  
395 incubation (Gazeau et al., 2020). The coccolithophore *Emiliana huxleyi* appears as one of the  
396 potential host candidates for these Giruses. The abundance of *E. huxleyi* increased in D and G at  
397 this station and this phytoplankter is known to be infected by such giant viruses (Jacquet et al.,  
398 2002; Schroeder et al., 2002; Pagarete et al., 2011). It is not clear from our results whether  
399 increased Girus abundance is due to the greenhouse effect only (as discussed above for viruses of  
400 HB) or the combination of dust addition and greenhouse effects. While temperature warming  
401 was shown to accelerate viral production in several virus – phytoplankton systems (Mojica and



402 Brussaard 2014, Demory et al. 2017), a temperature-induced resistance to viral infection was  
403 specifically observed in *E. huxleyi* (Kendrick et al., 2014). Previous experiments have also  
404 reported a negative impact of acidification on *E. huxleyi* virus dynamics (Larsen et al., 2008). By  
405 contrast, nutrient release following dust seeding could indirectly stimulate *E. huxleyi* virus  
406 production (Bratbak et al., 1993) or induced switching between non-lethal temperate to lethal  
407 lytic stage (Knowles et al., 2020) under future conditions. Targeted analyses are of course  
408 required to identify the viral populations selected in G and the outcomes of their infection.  
409 Nonetheless, this is the first time, to our knowledge, that dust deposition and enhanced  
410 temperature and acidification have been shown to induce the proliferation of G viruses. The impact  
411 of dust deposition under future environmental conditions on the viral infections processes could  
412 have significant consequences for microbial evolution, food web processes, biogeochemical  
413 cycles, and carbon sequestration.

414

#### 415 4.3 Microbial community dynamic after dust addition under present and future conditions

416 While changes in bacterial community composition during various type of dust addition  
417 experiments have shown only minor transient responses (e.g., Marañon et al., 2010; Hill et al.,  
418 2010; Laghdass et al., 2011; Pulido-Villena et al., 2014; Marín-Beltrán et al., 2019), here  
419 microbial community structure showed quick, significant and sustained changes in response to  
420 dust addition in all three experiments. Similar to other parameters observed during these  
421 experiments (discussed above and in Gazeau et al., 2020; Gazeau et al., 2021), the degree of  
422 response in terms of community composition was specific to the tested waters.



423 At TYR, where primary production was low, only transient changes after 24 h of incubation  
424 were observed, before the micro-eukaryotes community converged back close to initial  
425 conditions. In contrast, the bacterial community significantly and rapidly changed after 24 h and  
426 remained different after 72 h. At FAST, where the addition of dust appeared to promote  
427 autotrophic processes, the micro-eukaryotes community responded quickly 24 h after dust  
428 addition, while minor and delayed changes, probably related to the lower BP growth rates  
429 compared to the other tested waters, were observed in the bacterial community. At ION both  
430 eukaryotes and bacterial community responded to dust addition. The delayed response of micro-  
431 eukaryotes after 72 h compared to the quick bacterial response at 24 h suggests that HB were  
432 better at competing for nutrient inputs at this station and that autotrophic processes may be  
433 responding to bacterial nutrient regeneration after a lag phase, further suggesting the tight  
434 coupling between heterotrophic bacteria and phytoplankton at this station. The combined effect  
435 of decreased pH and elevated temperature on marine microbes is not yet well understood  
436 (reviewed in O'Brien et al., 2016). The absence of significant community changes at TYR and  
437 FAST while changes were observed at ION, suggests that the response might be dependent on  
438 other environmental factors, which need to be further studied.

439 Dust addition likely favors certain group of micro-organisms, suggesting a quicker response  
440 of fast growing/copiotrophic groups as well as the increase of specialized functional groups (Guo  
441 et al., 2016; Westrich et al., 2016; Maki et al., 2016). Potential toxicity effects of metals released  
442 from dust/aerosols on certain micro-organisms have also been reported (Paytan et al., 2009;  
443 Rahav et al., 2020). Here, the micro-eukaryotic community was dominated by a diverse group of  
444 dinoflagellates which were responsible for the main variations between treatments at all stations.  
445 The overwhelming abundance of dinoflagellates sequences over other micro-eukaryotes could be



446 biased by the large genomes and multiple ribosomal gene copies per genome found in  
447 dinoflagellates (Zhu et al., 2005) or due to their preferential amplification. However, the  
448 dominance of dinoflagellates in surface water at this time of the year in the Mediterranean Sea is  
449 not uncommon (García-Gómez et al., 2020) and was also observed in surface waters of the three  
450 sampled stations by Imaging Flow Cytobot (Marañón et al., 2021). While pigment data suggest  
451 an increase of haptophytes and pelagophytes in D (Gazeau et al., 2020), the sequencing data only  
452 show the presence of *Emiliana huxleyi* as responsible for some of the community changes after  
453 dust addition at ION and FAST. These pigments could also indicate the presence of  
454 dinoflagellates through tertiary endosymbiosis, in particular *Karlodinium* sp. (Yoon et al., 2002;  
455 Zapata et al., 2012), which is an important mixotrophic dinoflagellate (Calbet et al., 2011)  
456 observed in D and G at ION and FAST. The variations in dinoflagellate groups might have  
457 important trophic impacts due to their diverse mixotrophic states (Stoecker et al., 2017) and the  
458 effect of dust addition on mixotrophic interactions should be further studied to better understand  
459 the cascading impact of dust on food webs and the biological pump.

460 Positive to toxic impacts on cyanobacteria have been reported from atmospheric deposition  
461 experiments (e.g., Paytan et al., 2009; Zhou et al., 2021). Here, *Synechococcus* appeared to be  
462 inhibited at TYR while it was enhanced at ION and FAST, especially under future conditions  
463 (this study, Gazeau et al., 2020). The same ASVs appeared to be inhibited at TYR and ION  
464 while promoted at FAST and a different ASVs increased at ION. *Synechococcus* has recently  
465 been shown to be stimulated by wet aerosol addition in P-limited conditions but inhibited in N-  
466 limited conditions, in the South China Sea (Zhou et al., 2021). It was also shown to be repressed  
467 by dust addition in nutrient limited tropical Atlantic (Marañón et al., 2010). This suggests that



468 different *Synechococcus* ecotypes (Sohm et al., 2016) might respond differently to dust addition  
469 depending on the initial biogeochemical conditions of the water.

470 In the three experiments, the main bacterial ASVs responsible for the differences between  
471 the control and treatments were closely related to different *Alteromonas* strains. *Alteromonas* are  
472 ubiquitous in marine environment and can respond rapidly to nutrient pulses (López-Pérez and  
473 Rodríguez-Valera, 2014). Some *Alteromonas* are capable to grow on a wide range of carbon  
474 compounds (Pedler et al., 2014). They can produce iron binding ligands (Hogle et al., 2016) to  
475 rapidly assimilate Fe released from dust. Thus, they could have significant consequences for the  
476 marine carbon and Fe cycles during dust deposition events. Other copiotrophic  $\gamma$ -Proteobacteria,  
477 such as *Vibrio*, have been observed to bloom after dust deposition in the Atlantic Ocean  
478 (Westrich et al., 2016). Guo et al. (2016) using RNA sequencing, also show that  $\gamma$ -Proteobacteria  
479 quickly outcompete  $\alpha$ -Proteobacteria (mainly SAR11 and Rhodobacterales) that were initially  
480 more active. Here, while SAR11 relative abundance decreased in all experiments after 24h, other  
481  $\alpha$ -Proteobacteria related to the aerobic anoxygenic phototroph (AAP) *Erythrobacter* sp.,  
482 increased in response to dust, in particular under future conditions. Other AAP, such as OM60,  
483 also responded to dust addition in our experiment and in the Eastern Mediterranean Sea (Guo et  
484 al., 2016). Fast growing AAP might quickly outcompete other HB by supplementing their  
485 growth with light derived energy (e.g., Koblížek, 2015). They have also been shown to be  
486 stimulated by higher temperature (Sato-Takabe et al., 2019). AAP response to dust and future  
487 conditions could have a significant role in marine biogeochemical cycles.

## 488 5. Conclusion

489 The microbial food web response to dust addition was dependent on the initial state of the  
490 microbial community in the tested waters. A different response in trophic interactions and



491 community composition of the microbial food web, to the wet dust addition, was observed at  
492 each station. Generally greater changes were observed in future conditions. Pulsed input of  
493 nutrients and trace metals changed the microbial ecosystem from bottom-up limited to a top-  
494 down controlled bacterial community, likely from grazing and induced lysogeny. The  
495 composition of mixotrophic microeukaryotes and phototrophic prokaryotes was also altered.

496 Overall, the impact of such simulated pulsed nutrient deposition will depend on the initial  
497 biogeochemical conditions of the ecosystem, with likely possible large impact on microbial  
498 trophic interactions and community structure. All effects might be generally enhanced in future  
499 climate scenarios. The impact of dust deposition on metabolic processes and consequences for  
500 the carbon and nitrogen cycles and the biological pump based on these minicosm experiments  
501 are further discussed in Gazeau et al. (2021), and the *in situ* effect of a wet dust deposition event  
502 is explored in Van Wambeke et al. (2020), in this special issue.

## 503 **6. Data availability**

504 Guieu et al., Biogeochemical dataset collected during the PEACETIME cruise. SEANOE.  
505 <https://doi.org/10.17882/75747> (2020). All sequences associated with this study have been  
506 deposited under the BioProject ID: PRJNA693966.

## 507 508 **7. Author contributions**

509 FG and CG designed the experiment. All authors participated in sampling or sample  
510 processes. JD analyzed the data and wrote the paper with contributions from all authors.

## 511 **8. Competing interests**

512 The authors declare that they have no conflict of interest.





513 **9. Special issue statement**

514 This article is part of the special issue ‘Atmospheric deposition in the low-nutrient–low-  
515 chlorophyll (LNLC) ocean: effects on marine life today and in the future (ACP/BG inter-  
516 journal SI)’. It is not associated with a conference.

517 **10. Financial support**

518 Part of this research was funded by the ANR CALYPSO attributed to ACB (ANR-15-CE01-  
519 0009). EM was supported by the Spanish Ministry of Science, Innovation and Universities  
520 through grant PGC2018-094553B-I00. JD was funded by a Marie Curie Actions-International  
521 Outgoing Fellowship (PIOF-GA-2013-629378).

522

523 **11. Acknowledgements**

524 This study is a contribution to the PEACETIME project (<http://peacetime-project.org>,  
525 <https://doi.org/10.17600/17000300>), a joint initiative of the MERMEX and ChArMEX  
526 components supported by CNRS-INSU, IFREMER, CEA, and Météo-France as part of the  
527 programme MISTRALS coordinated by INSU. PEACETIME was endorsed as a process study  
528 by GEOTRACES and is also a contribution to SOLAS. We gratefully acknowledge the onboard  
529 support from the captain and crew of the RV Pourquoi Pas? and of our chief scientists C. Guieu  
530 and K. Desboeufs. We also thank K. Djaoudi for her assistance in sampling the minicosms, P.  
531 Catala, B. Marie and M. Perez-Lorenzo with their assistance in measuring microbial abundance,  
532 DOC concentration and primary production.

533

534 **12. References**



535 Allen, R., Hoffmann, L. J., Law, C. S., and Summerfield, T. C.: Subtle bacterioplankton  
536 community responses to elevated CO<sub>2</sub> and warming in the oligotrophic South Pacific gyre, *Env*  
537 *Microbiol Rep*, 12, 377-386, <https://doi.org/10.1111/1758-2229.12844>, 2020.

538 Bolyen, E., Rideout, J. R., Dillon, M. R., Bokulich, N. A., Abnet, C. C., Al-Ghalith, G. A.,  
539 Alexander, H., Alm, E. J., Arumugam, M., Asnicar, F., Bai, Y., Bisanz, J. E., Bittinger, K.,  
540 Brejnrod, A., Brislawn, C. J., Brown, C. T., Callahan, B. J., Caraballo-Rodríguez, A. M.,  
541 Chase, J., Cope, E. K., Da Silva, R., Diener, C., Dorrestein, P. C., Douglas, G. M., Durall, D.  
542 M., Duvallet, C., Edwardson, C. F., Ernst, M., Estaki, M., Fouquier, J., Gauglitz, J. M.,  
543 Gibbons, S. M., Gibson, D. L., Gonzalez, A., Gorlick, K., Guo, J., Hillmann, B., Holmes, S.,  
544 Holste, H., Huttenhower, C., Huttley, G. A., Janssen, S., Jarmusch, A. K., Jiang, L., Kaehler,  
545 B. D., Kang, K. B., Keefe, C. R., Keim, P., Kelley, S. T., Knights, D., Koester, I., Kosciulek,  
546 T., Kreps, J., Langille, M. G. I., Lee, J., Ley, R., Liu, Y.-X., Loftfield, E., Lozupone, C.,  
547 Maher, M., Marotz, C., Martin, B. D., McDonald, D., McIver, L. J., Melnik, A. V., Metcalf, J.  
548 L., Morgan, S. C., Morton, J. T., Naimey, A. T., Navas-Molina, J. A., Nothias, L. F.,  
549 Orchanian, S. B., Pearson, T., Peoples, S. L., Petras, D., Preuss, M. L., Pruesse, E., Rasmussen,  
550 L. B., Rivers, A., Robeson, M. S., Rosenthal, P., Segata, N., Shaffer, M., Shiffer, A., Sinha, R.,  
551 Song, S. J., Spear, J. R., Swafford, A. D., Thompson, L. R., Torres, P. J., Trinh, P., Tripathi,  
552 A., Turnbaugh, P. J., Ul-Hasan, S., van der Hoof, J. J. J., Vargas, F., Vázquez-Baeza, Y.,  
553 Vogtmann, E., von Hippel, M., Walters, W., Wan, Y., Wang, M., Warren, J., Weber, K. C.,  
554 Williamson, C. H. D., Willis, A. D., Xu, Z. Z., Zaneveld, J. R., Zhang, Y., Zhu, Q., Knight, R.,  
555 and Caporaso, J. G.: Reproducible, interactive, scalable and extensible microbiome data  
556 science using QIIME 2, *Nat Biotechnol*, 37, 852-857, [10.1038/s41587-019-0209-9](https://doi.org/10.1038/s41587-019-0209-9), 2019.



- 557 Bonnet, S., and Guieu, C.: Atmospheric forcing on the annual iron cycle in the Western  
558 Mediterranean Sea: A 1-year survey, *J Geophys Res-Oceans*, 111,  
559 <https://doi.org/10.1029/2005JC003213>, 2006.
- 560 Bosc, E., Bricaud, A., and Antoine, D.: Seasonal and interannual variability in algal biomass and  
561 primary production in the Mediterranean Sea, as derived from 4 years of SeaWiFS  
562 observations, *Global Biogeochem Cy*, 18, <https://doi.org/10.1029/2003GB002034>, 2004.
- 563 Bratbak, G., Egge, J. K., and Heldal, M.: Viral mortality of the marine alga *Emiliania huxleyi*  
564 (Haptophyceae) and termination of algal blooms, *Mar Ecol Prog Ser*, 39-48, 1993.
- 565 Brussaard, C., Noordeloos, A., Witte, H., Collenteur, M., Schulz, K. G., Ludwig, A., and  
566 Riebesell, U.: Arctic microbial community dynamics influenced by elevated CO<sub>2</sub> levels,  
567 *Biogeosciences*, 10, 719-731, 2013.
- 568 Brussaard, C. P., and Martinez, J. M.: Algal bloom viruses, *Plant Viruses*, 2, 1-13, 2008.
- 569 Brussaard, C. P. D.: Optimization of Procedures for Counting Viruses by Flow Cytometry, *Appl*  
570 *Environ Microb*, 70, 1506-1513, [10.1128/aem.70.3.1506-1513.2004](https://doi.org/10.1128/aem.70.3.1506-1513.2004), 2004.
- 571 Calbet, A., Bertos, M., Fuentes-Grünwald, C., Alacid, E., Figueroa, R., Renom, B., and Garcés,  
572 E.: Intraspecific variability in *Karlodinium veneficum*: growth rates, mixotrophy, and lipid  
573 composition, *Harmful Algae*, 10, 654-667, 2011.
- 574 Callahan, B. J., McMurdie, P. J., Rosen, M. J., Han, A. W., Johnson, A. J. A., and Holmes, S. P.:  
575 DADA2: High-resolution sample inference from Illumina amplicon data, *Nat Methods*, 13,  
576 581, [10.1038/nmeth.3869](https://doi.org/10.1038/nmeth.3869), 2016.
- 577 Clarke, K. R., and Warwick, P. E.: *Change in Marine Communities: An Approach to Statistical*  
578 *Analysis and Interpretation*, Plymouth, Ltd ed., 2001.



- 579 D'Ortenzio, F., Iudicone, D., de Boyer Montegut, C., Testor, P., Antoine, D., Marullo, S.,  
580 Santoleri, R., and Madec, G.: Seasonal variability of the mixed layer depth in the  
581 Mediterranean Sea as derived from *in situ* profiles, *Geophys Res Let*, 32,  
582 <https://doi.org/10.1029/2005GL022463>, 2005.
- 583 Danovaro, R., Corinaldesi, C., Dell'Anno, A., Fuhrman, J. A., Middelburg, J. J., Noble, R. T.,  
584 and Suttle, C. A.: Marine viruses and global climate change, *FEMS Microbiol Rev*, 35, 993-  
585 1034, [10.1111/j.1574-6976.2010.00258.x](https://doi.org/10.1111/j.1574-6976.2010.00258.x), 2011.
- 586 Degerman, R., Dinasquet, J., Riemann, L., Sjostedt de Luna, S., and Andersson, A.: Effect of  
587 resource availability on bacterial community responses to increased temperature, *Aquat Microb*  
588 *Ecol*, 68: 131-142, 2012.
- 589 Desboeufs, K., Leblond, N., Wagener, T., Bon Nguyen, E., and Guieu, C.: Chemical fate and  
590 settling of mineral dust in surface seawater after atmospheric deposition observed from dust  
591 seeding experiments in large mesocosms, *Biogeosciences*, 11, 5581-5594, [10.5194/bg-11-](https://doi.org/10.5194/bg-11-5581-2014)  
592 [5581-2014](https://doi.org/10.5194/bg-11-5581-2014), 2014.
- 593 Ducklow, H.: Factors regulating bottom-up control of bacteria biomass in open ocean plankton  
594 communities, *Arch. Hydrobiol. Beih. Ergebn. Limnol*, 37, 207-217, 1992.
- 595 Durrieu de Madron, X., Guieu, C., Sempéré, R., Conan, P., Cossa, D., D'Ortenzio, F., Estournel,  
596 C., Gazeau, F., Rabouille, C., Stemmann, L., Bonnet, S., Diaz, F., Koubbi, P., Radakovitch, O.,  
597 Babin, M., Baklouti, M., Bancon-Montigny, C., Belviso, S., Bensoussan, N., Bonsang, B.,  
598 Bouloubassi, I., Brunet, C., Cadiou, J. F., Carlotti, F., Chami, M., Charmasson, S., Charrière,  
599 B., Dachs, J., Doxaran, D., Dutay, J. C., Elbaz-Poulichet, F., Eléaume, M., Eyrolles, F.,  
600 Fernandez, C., Fowler, S., Francour, P., Gaertner, J. C., Galzin, R., Gasparini, S., Ghiglione, J.  
601 F., Gonzalez, J. L., Goyet, C., Guidi, L., Guizien, K., Heimbürger, L. E., Jacquet, S. H. M.,



602 Jeffrey, W. H., Joux, F., Le Hir, P., Leblanc, K., Lefèvre, D., Lejeusne, C., Lemé, R., Loÿe-  
603 Pilot, M. D., Mallet, M., Méjanelle, L., Mélin, F., Mellon, C., Mérigot, B., Merle, P. L., Migon,  
604 C., Miller, W. L., Mortier, L., Mostajir, B., Mousseau, L., Moutin, T., Para, J., Pérez, T.,  
605 Petrenko, A., Poggiale, J. C., Prieur, L., Pujo-Pay, M., Pulido, V., Raimbault, P., Rees, A. P.,  
606 Ridame, C., Rontani, J. F., Ruiz Pino, D., Sicre, M. A., Taillandier, V., Tamburini, C., Tanaka,  
607 T., Taupier-Letage, I., Tedetti, M., Testor, P., Thébault, H., Thouvenin, B., Touratier, F.,  
608 Tronczynski, J., Ulses, C., Van Wambeke, F., Vantrepotte, V., Vaz, S., and Verney, R.: Marine  
609 ecosystems' responses to climatic and anthropogenic forcings in the Mediterranean, *Prog*  
610 *Oceanog*, 91, 97-166, <https://doi.org/10.1016/j.pocean.2011.02.003>, 2011.

611 Fischer, M. G., Allen, M. J., Wilson, W. H., and Suttle, C. A.: Giant virus with a remarkable  
612 complement of genes infects marine zooplankton, *P Natl Acad Sci* 107, 19508-19513, 2010.

613 García-Gómez, C., Yebra, L., Cortés, D., Sánchez, A., Alonso, A., Valcárcel-Pérez, N., Gómez-  
614 Jakobsen, F., Herrera, I., Johnstone, C., and Mercado, J. M.: Shifts in the protist community  
615 associated with an anticyclonic gyre in the Alboran Sea (Mediterranean Sea), *FEMS Microbiol*  
616 *Ecol*, 96, 10.1093/femsec/fiaa197, 2020.

617 Gasol, J. M.: A framework for the assessment of top-down vs bottom-up control of heterotrophic  
618 nanoflagellate abundance, *Mar ecol prog ser.* 113, 291-300, 1994.

619 Gazeau, F., Ridame, C., Van Wambeke, F., Alliouane, S., Stolpe, C., Irisson, J. O., Marro, S.,  
620 Grisoni, J. M., De Liège, G., Nunige, S., Djaoudi, K., Pulido-Villena, E., Dinasquet, J.,  
621 Obermosterer, I., Catala, P., and Guieu, C.: Impact of dust enrichment on Mediterranean  
622 plankton communities under present and future conditions of pH and temperature: an  
623 experimental overview, *Biogeosciences Discuss.*, 2020, 1-81, 10.5194/bg-2020-202, 2020.



- 624 Gazeau, F., Van Wambeke, F., Marañón, E., Pérez-Lorenzo, M., Alliouane, S., Stolpe, C.,  
625 Blasco, T., Leblond, N., Zäncker, B., Engel, A., Marie, B., Dinasquet, J., and Guieu, C.: Impact  
626 of dust addition on the metabolism of Mediterranean plankton communities and carbon export  
627 under present and future conditions of pH and temperature, *Biogeosciences Discuss.*,  
628 <https://doi.org/10.5194/bg-2021-20>, in review, 2021.
- 629 Guieu, C., Aumont, O., Paytan, A., Bopp, L., Law, C. S., Mahowald, N., Achterberg, E. P.,  
630 Marañón, E., Salihoglu, B., Crise, A., Wagener, T., Herut, B., Desboeufs, K., Kanakidou, M.,  
631 Olgun, N., Peters, F., Pulido-Villena, E., Tovar-Sanchez, A., and Völker, C.: The significance  
632 of the episodic nature of atmospheric deposition to Low Nutrient Low Chlorophyll regions,  
633 *Global Biogeochem Cy*, 28, 1179-1198, 10.1002/2014GB004852, 2014.
- 634 Guieu, C. and Ridame, C.: Impact of atmospheric deposition on marine chemistry and  
635 biogeochemistry, in *Atmospheric Chemistry in the Mediterranean Region: Comprehensive  
636 Diagnosis and Impacts*, edited by F. Dulac, S. Sauvage, and E. Hamonou, Springer, Cham,  
637 Switzerland, 2020.
- 638 Guillou, L., Bachar, D., Audic, S., Bass, D., Berney, C., Bittner, L., Boutte, C., Burgaud, G., de  
639 Vargas, C., Decelle, J., del Campo, J., Dolan, J. R., Dunthorn, M., Edvardsen, B., Holzmann,  
640 M., Kooistra, W. H. C. F., Lara, E., Le Bescot, N., Logares, R., Mahé, F., Massana, R.,  
641 Montresor, M., Morard, R., Not, F., Pawlowski, J., Probert, I., Sauvadet, A.-L., Siano, R.,  
642 Stoeck, T., Vaulot, D., Zimmermann, P., and Christen, R.: The Protist Ribosomal Reference  
643 database (PR2): a catalog of unicellular eukaryote Small Sub-Unit rRNA sequences with  
644 curated taxonomy, *Nucleic Acids Res*, 41, D597-D604, 10.1093/nar/gks1160, 2013.
- 645 Guo, C., Xia, X., Pitta, P., Herut, B., Rahav, E., Berman-Frank, I., Giannakourou, A., Tsiola, A.,  
646 Tsagaraki, T. M., and Liu, H.: Shifts in Microbial Community Structure and Activity in the



- 647 Ultra-Oligotrophic Eastern Mediterranean Sea Driven by the Deposition of Saharan Dust and  
648 European Aerosols, *Front Mar Sci*, 3, 10.3389/fmars.2016.00170, 2016.
- 649 Highfield, A., Joint, I., Gilbert, J. A., Crawford, K. J., and Schroeder, D. C.: Change in *Emiliana*  
650 *huxleyi* Virus Assemblage Diversity but Not in Host Genetic Composition during an Ocean  
651 Acidification Mesocosm Experiment, *Viruses*, 9, 41, 2017.
- 652 Hill, P. G., Zubkov, M. V., and Purdie, D. A.: Differential responses of *Prochlorococcus* and  
653 SAR11-dominated bacterioplankton groups to atmospheric dust inputs in the tropical Northeast  
654 Atlantic Ocean, *FEMS Microbiol Let*, 306, 82-89, 10.1111/j.1574-6968.2010.01940.x, 2010.
- 655 Hogle, S. L., Bundy, R. M., Blanton, J. M., Allen, E. E., and Barbeau, K. A.: Copiotrophic  
656 marine bacteria are associated with strong iron-binding ligand production during  
657 phytoplankton blooms, *Limnol Oceanogr Let*, 10.1002/lol2.10026, 2016.
- 658 Hu, C., Li, X., He, M., Jiang, P., Long, A., and Xu, J.: Effect of Ocean Acidification on Bacterial  
659 Metabolic Activity and Community Composition in Oligotrophic Oceans, Inferred From Short-  
660 Term Bioassays, *Front Microbiol*, 12, 10.3389/fmicb.2021.583982, 2021.
- 661 IPCC: Climate Change 2013: The Physical Science Basis. Contribution of Working Group I to  
662 the Fifth Assessment Report of the Intergovernmental Panel on Climate Change, Cambridge  
663 University Press, Cambridge, United Kingdom and New York, NY, USA, 1535 pp., 2014.
- 664 Jacquet, S., Heldal, M., Iglesias-Rodriguez, D., Larsen, A., Wilson, W., and Bratbak, G.: Flow  
665 cytometric analysis of an *Emiliana huxleyi* bloom terminated by viral infection, *Aquat Microb*  
666 *Ecol*, 27, 111-124, 2002.
- 667 Kendrick, B. J., DiTullio, G. R., Cyronak, T. J., Fulton, J. M., Van Mooy, B. A., and Bidle, K.  
668 D.: Temperature-induced viral resistance in *Emiliana huxleyi* (Prymnesiophyceae), *PLoS One*,  
669 9, e112134, 2014.



670 Kirchman, D., Knees, E., and Hodson, R.: Leucine Incorporation and Its Potential As A Measure  
671 of Protein-Synthesis by Bacteria in Natural Aquatic Systems, *Appl Environ Microbiol*, 49,  
672 599-607, 1985.

673 Knowles, B., Bonachela, J. A., Behrenfeld, M. J., Bondoc, K. G., Cael, B., Carlson, C. A.,  
674 Cieslik, N., Diaz, B., Fuchs, H. L., and Graff, J. R.: Temperate infection in a virus–host system  
675 previously known for virulent dynamics, *Nat comms*, 11, 1-13, 2020.

676 Koblížek, M.: Ecology of aerobic anoxygenic phototrophs in aquatic environments, *FEMS*  
677 *Microbiol Rev*, 39, 854-870, 10.1093/femsre/fuv032, 2015.

678 Krause, E., Wichels, A., Giménez, L., Lunau, M., Schilhabel, M. B., and Gerdts, G.: Small  
679 Changes in pH Have Direct Effects on Marine Bacterial Community Composition: A  
680 Microcosm Approach, *PLOS ONE*, 7, e47035, 10.1371/journal.pone.0047035, 2012.

681 Laghdass, M., Blain, S., Besseling, M., Catala, P., Guieu, C., and Obernosterer, I.: Effects of  
682 Saharan dust on the microbial community during a large *in situ* mesocosm experiment in the  
683 NW Mediterranean Sea, *Aquat Microb Ecol*, 62, 201-213, 2011.

684 Larsen, J. B., Larsen, A., Thyrraug, R., Bratbak, G., and Sandaa, R.-A.: Response of marine  
685 viral populations to a nutrient induced phytoplankton bloom at different  $p\text{CO}_2$  levels,  
686 *Biogeosciences*, 5, 523-533, 2008.

687 Lee, S. H., and Fuhrman, J. A.: Relationships between biovolume and biomass of naturally  
688 derived marine bacterioplankton, *Appl Environ Microbiol*, 53, 1298-1303, 1987.

689 Loÿe-Pilot, M., and Martin, J.: Saharan dust input to the western Mediterranean: an eleven years  
690 record in Corsica, in: *The impact of desert dust across the Mediterranean*, Springer, 191-199,  
691 1996.





- 692 López-Pérez, M., and Rodriguez-Valera, F.: The Family Alteromonadaceae, in: The Prokaryotes:  
693 Gammaproteobacteria, edited by: Rosenberg, E., DeLong, E. F., Lory, S., Stackebrandt, E., and  
694 Thompson, F., Springer Berlin Heidelberg, Berlin, Heidelberg, 69-92, 2014.
- 695 Maat, D. S., Crawford, K. J., Timmermans, K. R., and Brussaard, C. P.: Elevated carbon dioxide  
696 and phosphorus limitation favor *Micromonas pusilla* through stimulated growth and reduced  
697 viral impact, aspects of algal host-virus interactions in a changing ocean, 80, 29, 2014.
- 698 Mahowald, N. M., Scanza, R., Brahney, J., Goodale, C. L., Hess, P. G., Moore, J. K., and Neff,  
699 J.: Aerosol Deposition Impacts on Land and Ocean Carbon Cycles, Current Climate Change  
700 Reports, 3, 16-31, 10.1007/s40641-017-0056-z, 2017.
- 701 Maki, T., Ishikawa, A., Mastunaga, T., Pointing, S. B., Saito, Y., Kasai, T., Watanabe, K., Aoki,  
702 K., Horiuchi, A., Lee, K. C., Hasegawa, H., and Iwasaka, Y.: Atmospheric aerosol deposition  
703 influences marine microbial communities in oligotrophic surface waters of the western Pacific  
704 Ocean, Deep Sea Research Part I: Oceanographic Research Papers, 118, 37-45,  
705 <https://doi.org/10.1016/j.dsr.2016.10.002>, 2016.
- 706 Malits, A., Boras, J.A., Balagué, V., Calvo, E., Gasol, J.M., Marrasé, C., Pelejero, C., Pinhassi,  
707 J., Sala, M.M. and Vaqué, D. Viral-Mediated Microbe Mortality Modulated by Ocean  
708 Acidification and Eutrophication: Consequences for the Carbon Fluxes Through the Microbial  
709 Food Web. *Front. Microbiol.* 12:635821. doi: 10.3389/fmicb.2021.635821, 2021
- 710 Marañón, E., Fernández, A., Mouriño-Carballido, B., Martínez-García, S., Teira, E., Cermeño,  
711 P., Chouciño, P., Huete-Ortega, M., Fernández, E., Calvo-Díaz, A., Morán, X. A. G., Bode, A.,  
712 Moreno-Ostos, E., Varela, M. M., Patey, M. D., and Achterberg, E. P.: Degree of oligotrophy  
713 controls the response of microbial plankton to Saharan dust, *Limnology and Oceanography*, 55,  
714 2339-2352, <https://doi.org/10.4319/lo.2010.55.6.2339>, 2010.



- 715 Marañón, E., Lorenzo, M. P., Cermeño, P., and Mouriño-Carballido, B.: Nutrient limitation  
716 suppresses the temperature dependence of phytoplankton metabolic rates, *The ISME Journal*,  
717 12, 1836-1845, 10.1038/s41396-018-0105-1, 2018.
- 718 Marañón, E., Van Wambeke, F., Uitz, J., Boss, E. S., Pérez-Lorenzo, M., Dinasquet, J.,  
719 Haëntjens, N., Dimier, C., and Taillandier, V.: Deep maxima of phytoplankton biomass,  
720 primary production and bacterial production in the Mediterranean Sea during late spring,  
721 *Biogeosciences*, 18, 1749–1767, <https://doi.org/10.5194/bg-18-1749-2021>, 2021
- 722 Marín-Beltrán, I., Logue, J. B., Andersson, A. F., and Peters, F.: Atmospheric Deposition Impact  
723 on Bacterial Community Composition in the NW Mediterranean, *Frontiers in Microbiology*,  
724 10, 10.3389/fmicb.2019.00858, 2019.
- 725 Martínez, J. M., Swan, B. K., and Wilson, W. H.: Marine viruses, a genetic reservoir revealed by  
726 targeted viromics, *The ISME Journal*, 8, 1079-1088, 10.1038/ismej.2013.214, 2014.
- 727 Mojica, K. D., and Brussaard, C. P.: Factors affecting virus dynamics and microbial host–virus  
728 interactions in marine environments, *FEMS microbiology ecology*, 89, 495-515, 2014.
- 729 Morán, X. A. G., Gasol, J. M., Pernice, M. C., Mangot, J.-F., Massana, R., Lara, E., Vaqué, D.,  
730 and Duarte, C. M.: Temperature regulation of marine heterotrophic prokaryotes increases  
731 latitudinally as a breach between bottom-up and top-down controls, *Global Change Biology*,  
732 23, 3956-3964, <https://doi.org/10.1111/gcb.13730>, 2017.
- 733 Morán, X. A. G., Baltar, F., Carreira, C., and Lønborg, C.: Responses of physiological groups of  
734 tropical heterotrophic bacteria to temperature and dissolved organic matter additions: food  
735 matters more than warming, *Environmental Microbiology*, 22, 1930-1943,  
736 <https://doi.org/10.1111/1462-2920.15007>, 2020.



- 737 Moulin, C., and Chiapello, I.: Impact of human-induced desertification on the intensification of  
738 Sahel dust emission and export over the last decades, *Geophysical Research Letters*, 33,  
739 <https://doi.org/10.1029/2006GL025923>, 2006.
- 740 Needham, D. M., Yoshizawa, S., Hosaka, T., Poirier, C., Choi, C. J., Hehenberger, E., Irwin, N.  
741 A., Wilken, S., Yung, C.-M., and Bachy, C.: A distinct lineage of giant viruses brings a  
742 rhodopsin photosystem to unicellular marine predators, *Proceedings of the National Academy*  
743 *of Sciences*, 116, 20574-20583, 2019.
- 744 O'Brien, P. A., Morrow, K. M., Willis, B. L., and Bourne, D. G.: Implications of Ocean  
745 Acidification for Marine Microorganisms from the Free-Living to the Host-Associated,  
746 *Frontiers in Marine Science*, 3, 10.3389/fmars.2016.00047, 2016.
- 747 Pagarete, A., Le Corguillé, G., Tiwari, B., Ogata, H., de Vargas, C., Wilson, W. H., and Allen,  
748 M. J.: Unveiling the transcriptional features associated with coccolithovirus infection of natural  
749 *Emiliana huxleyi* blooms, *FEMS Microbiology Ecology*, 78, 555-564, 10.1111/j.1574-  
750 6941.2011.01191.x, 2011.
- 751 Parada, A. E., Needham, D. M., and Fuhrman, J. A.: Every base matters: assessing small subunit  
752 rRNA primers for marine microbiomes with mock communities, time series and global field  
753 samples, *Environmental Microbiology*, 18, 1403-1414, 10.1111/1462-2920.13023, 2016.
- 754 Parada, V., Herndl, G. J., and Weinbauer, M. G.: Viral burst size of heterotrophic prokaryotes in  
755 aquatic systems, *JMBA-Journal of the Marine Biological Association of the United Kingdom*,  
756 86, 613, 2006.
- 757 Paytan, A., Mackey, K. R. M., Chen, Y., Lima, I. D., Doney, S. C., Mahowald, N., Labiosa, R.,  
758 and Post, A. F.: Toxicity of atmospheric aerosols on marine phytoplankton, *Proceedings of the*  
759 *National Academy of Sciences*, 106, 4601-4605, 10.1073/pnas.0811486106, 2009.



760 Pedler, B. E., Aluwihare, L. I., and Azam, F.: Single bacterial strain capable of significant  
761 contribution to carbon cycling in the surface ocean, *Proceedings of the National Academy of*  
762 *Sciences of the United States of America*, 111, 7202-7207, 2014.

763 Pinheiro, J., Bates, D., DebRoy, S., and Sarkar, D.: R Core Team. nlme: linear and nonlinear  
764 mixed effects models. R package version 3.1-117, Available at [http://CRAN.R-project.](http://CRAN.R-project.org/package=nlme)  
765 [org/package=nlme](http://CRAN.R-project.org/package=nlme), 2014.

766 Pitta, P., Kanakidou, M., Mihalopoulos, N., Christodoulaki, S., Dimitriou, P.D., Frangoulis, C.,  
767 Giannakourou, A., Kagiorgi, M., Lagaria, A., Nikolaou, P., Papageorgiou, N., Psarra, S., Santi,  
768 I., Tsapakis, M., Tsiola, A., Violaki, K., and Petihakis, G. Saharan Dust Deposition Effects on  
769 the Microbial Food Web in the Eastern Mediterranean: A Study Based on a Mesocosm  
770 Experiment. *Front. Mar. Sci.* 4:117. doi: 10.3389/fmars.2017.00117, 2017

771 Pulido-Villena, E., Baudoux, A. C., Obernosterer, I., Landa, M., Caparros, J., Catala, P.,  
772 Georges, C., Harmand, J., and Guieu, C.: Microbial food web dynamics in response to a  
773 Saharan dust event: results from a mesocosm study in the oligotrophic Mediterranean Sea,  
774 *Biogeosciences*, 11, 5607-5619, 10.5194/bg-11-5607-2014, 2014.

775 Quast, C., Pruesse, E., Yilmaz, P., Gerken, J., Schweer, T., Yarza, P., Peplies, J., and Glöckner,  
776 F. O.: The SILVA ribosomal RNA gene database project: improved data processing and web-  
777 based tools, *Nucleic Acids Research*, 41, D590-D596, 10.1093/nar/gks1219, 2013.

778 R Core Team: R: A language and environment for statistical computing. , R Foundation for  
779 Statistical Computing, Vienna, Austria., <https://www.R-project.org/>. 2020.

780 Rahav, E., Paytan, A., Mescioglou, E., Bar-Zeev, E., Martínez Ruiz, F., Xian, P., and Herut, B.:  
781 Bio-Aerosols Negatively Affect Prochlorococcus in Oligotrophic Aerosol-Rich Marine  
782 Regions, *Atmosphere*, 11, 540, 2020.



- 783 Ridame, C., Le Moal, M., Guieu, C., TERNON, E., Biegala, I. C., L'Helguen, S., and Pujo-Pay, M.:  
784 Nutrient control of N<sub>2</sub> fixation in the oligotrophic Mediterranean Sea and the impact of  
785 Saharan dust events, *Biogeosciences*, 8, 2773-2783, 10.5194/bg-8-2773-2011, 2011.
- 786 Sánchez, O., Ferrera, I., Mabrito, I., Gazulla, C. R., Sebastián, M., Auladell, A., Marín-Vindas,  
787 C., Cardelús, C., Sanz-Sáez, I., Pernice, M. C., Marrasé, C., Sala, M. M., and Gasol, J. M.:  
788 Seasonal impact of grazing, viral mortality, resource availability and light on the group-  
789 specific growth rates of coastal Mediterranean bacterioplankton, *Scientific Reports*, 10, 19773,  
790 10.1038/s41598-020-76590-5, 2020.
- 791 Sato-Takabe, Y., Hamasaki, K., and Suzuki, S.: High temperature accelerates growth of aerobic  
792 anoxygenic phototrophic bacteria in seawater, *MicrobiologyOpen*, 8, e00710-e00710,  
793 10.1002/mbo3.710, 2019.
- 794 Schroeder, D., Oke, J., Malin, G., and Wilson, W.: Coccolithovirus (Phycodnaviridae):  
795 characterisation of a new large dsDNA algal virus that infects *Emiliana huxleyi*, *Archives of*  
796 *virology*, 147, 1685-1698, 2002.
- 797 Siokou-Frangou, I., Christaki, U., Mazzocchi, M. G., Montresor, M., Ribera d'Alcalá, M., Vaqué,  
798 D., and Zingone, A.: Plankton in the open Mediterranean Sea: a review, *Biogeosciences*, 7,  
799 1543-1586, 10.5194/bg-7-1543-2010, 2010.
- 800 Smith, D. C., and Azam, F.: A simple, economical method for measuring bacterial protein  
801 synthesis rates in seawater using <sup>3</sup>H-leucine, *Marine microbial food webs*, 6, 102-114, 1992.
- 802 Sohm, J. A., Ahlgren, N. A., Thomson, Z. J., Williams, C., Moffett, J. W., Saito, M. A., Webb,  
803 E. A., and Rocap, G.: Co-occurring *Synechococcus* ecotypes occupy four major oceanic  
804 regimes defined by temperature, macronutrients and iron, *The ISME journal*, 10, 333-345,  
805 10.1038/ismej.2015.115, 2016.



- 806 Stoeck, T., Bass, D., Nebel, M., Christen, R., Jones, M. D. M., Breiner, H. W., and Richards, T.  
807 A.: Multiple marker parallel tag environmental DNA sequencing reveals a highly complex  
808 eukaryotic community in marine anoxic water, *Molecular Ecology*, 19, 21-31, 2010.
- 809 Stoecker, D. K., Hansen, P. J., Caron, D. A., and Mitra, A.: Mixotrophy in the Marine Plankton,  
810 *Annual Review of Marine Science*, 9, 311-335, 10.1146/annurev-marine-010816-060617,  
811 2017.
- 812 Suttle, C. A.: Marine viruses — major players in the global ecosystem, *Nature Reviews*  
813 *Microbiology*, 5, 801-812, 10.1038/nrmicro1750, 2007.
- 814 Ternon, E., Guieu, C., Loÿe-Pilot, M. D., Leblond, N., Bosc, E., Gasser, B., Miquel, J. C., and  
815 Martín, J.: The impact of Saharan dust on the particulate export in the water column of the  
816 North Western Mediterranean Sea, *Biogeosciences*, 7, 809-826, 10.5194/bg-7-809-2010, 2010.
- 817 Tsiola, A., Tsagaraki, T. M., Giannakourou, A., Nikolioudakis, N., Yücel, N., Herut, B., and  
818 Pitta, P.: Bacterial Growth and Mortality after Deposition of Saharan Dust and Mixed Aerosols  
819 in the Eastern Mediterranean Sea: A Mesocosm Experiment, *Frontiers in Marine Science*, 3,  
820 10.3389/fmars.2016.00281, 2017.
- 821 Van Wambeke, F., Taillandier, V., Deboeuufs, K., Pulido-Villena, E., Dinasquet, J., Engel, A.,  
822 Marañón, E., Ridame, C., and Guieu, C.: Influence of atmospheric deposition on  
823 biogeochemical cycles in an oligotrophic ocean system, *Biogeosciences Discuss.*, 2020, 1-51,  
824 10.5194/bg-2020-411.
- 825 Vaqué, D., Lara, E., Arrieta, J. M., Holding, J., Sarà, E. L., Hendriks, I. E., Coello-Camba, A.,  
826 Alvarez, M., Agustí, S., Wassmann, P. F., and Duarte, C. M.: Warming and CO<sub>2</sub> Enhance  
827 Arctic Heterotrophic Microbial Activity, *Frontiers in Microbiology*, 10,  
828 10.3389/fmicb.2019.00494, 2019.



- 829 Weinbauer, M., Bettarel, Y., Cattaneo, R., Luef, B., Maier, C., Motegi, C., Peduzzi, P., and Mari,  
830 X.: Viral ecology of organic and inorganic particles in aquatic systems: avenues for further  
831 research, *Aquatic Microbial Ecology*, 57, 321-341, 2009.
- 832 Weinbauer, M. G., Winter, C., and Höfle, M. G.: Reconsidering transmission electron  
833 microscopy based estimates of viral infection of bacterio-plankton using conversion factors  
834 derived from natural communities, *Aquatic Microbial Ecology*, 27, 103-110, 2002.
- 835 Weinbauer, M. G., Rowe, J. M., and Wilhelm, S.: Determining rates of virus production in  
836 aquatic systems by the virus reduction approach, 2010.
- 837 Westrich, J. R., Ebling, A. M., Landing, W. M., Joyner, J. L., Kemp, K. M., Griffin, D. W., and  
838 Lipp, E. K.: Saharan dust nutrients promote *Vibrio* bloom formation in marine surface waters,  
839 *Proceedings of the National Academy of Sciences*, 113, 5964-5969, 10.1073/pnas.1518080113,  
840 2016.
- 841 Winter, C., Herndl, G. J., and Weinbauer, M. G.: Diel cycles in viral infection of  
842 bacterioplankton in the North Sea, *Aquatic Microbial Ecology*, 35, 207-216, 2004.
- 843 Yamada, Y., Guillemette, R., Baudoux, A.-C., Patel, N., and Azam, F.: Viral Attachment to  
844 Biotic and Abiotic Surfaces in Seawater, *Applied and Environmental Microbiology*, 86,  
845 e01687-01619, 10.1128/aem.01687-19, 2020.
- 846 Yoon, H. S., Hackett, J. D., and Bhattacharya, D.: A single origin of the peridinin- and  
847 fucoxanthin-containing plastids in dinoflagellates through tertiary endosymbiosis, *Proceedings*  
848 *of the National Academy of Sciences*, 99, 11724-11729, 10.1073/pnas.172234799, 2002.
- 849 Zapata, M., Fraga, S., Rodríguez, F., and Garrido, J. L.: Pigment-based chloroplast types in  
850 dinoflagellates, *Marine Ecology Progress Series*, 465, 33-52, 2012.



851 Zhou, W., Li, Q. P., and Wu, Z.: Coastal phytoplankton responses to atmospheric deposition  
852 during summer, *Limnol Oceanogr*, 66: 1298-1315, 2021.

853 Zhu, F., Massana, R., Not, F., Marie, D., and Vaultot, D.: Mapping of picoeucaryotes in marine  
854 ecosystems with quantitative PCR of the 18S rRNA gene, *FEMS microbiology ecology*, 52,  
855 79-92, 2005.

856

857





858 **Tables and Figures**

859 **Table1:** Initial conditions (t-12h) at the three stations sampled for the dust addition experiments. Other  
 860 parameters are presented in more details in Gazeau et al. (2020; 2021)

Variables	TYR	ION	FAST
Location	Tyrrhenian Basin	Ionian Basin	Algerian Basin
Coordinates	39.34N, 12.60E	35.49N, 19.78E	37.95N, 2.90E
Temperatures (°C)	20.6	21.2	21.5
DOC (µM) <sup>2</sup>	72.2	70.2	69.6
Chlorophyll <i>a</i> (µg L <sup>-1</sup> ) <sup>1</sup>	0.063	0.066	0.072
BP (ng C L <sup>-1</sup> h <sup>-1</sup> ) <sup>2</sup>	11.6	15.1	34.6
Bacterial abundance (x10 <sup>5</sup> cells mL <sup>-1</sup> ) <sup>1</sup>	4.79	2.14	6.15
Viral abundance (x 10 <sup>6</sup> VLP mL <sup>-1</sup> )	3.01	1.44	2.79
% Lysogenic bacteria FLC	22.7	19.4	7.8
% Lytic bacteria FLIC	17.5	37.2	42.7
Viral production (x 10 <sup>4</sup> VLP mL <sup>-1</sup> h <sup>-1</sup> )	2.05	1.36	7.99
HNF abundance (cells mL <sup>-1</sup> ) <sup>1</sup>	110	53	126
Diatoms (cells L <sup>-1</sup> ) <sup>1</sup>	340	900	1460
Dinoflagellates (cells L <sup>-1</sup> ) <sup>1</sup>	2770	3000	3410
Ciliates (cells L <sup>-1</sup> ) <sup>1</sup>	270	380	770

861

862 DOC: dissolved organic carbon, \* BP: heterotrophic prokaryotic production, HNF: Heterotrophic  
 863 nanoflagellates

864 <sup>1</sup>Results presented in Gazeau et al. 2020

865 <sup>2</sup>Results presented in Gazeau et al. 2021

866

867



868 **Table 2.** Net growth rates ( $h^{-1}$ ) calculated from the exponential phase of growth of BP,  
 869 abundances of *Synechococcus* and picoeukaryotes cells, observable from at least three  
 870 successive sampling points. Values  $\pm$  standard error are shown, as well as the period of  
 871 exponential phase (period, in days). nd: no significant exponential phase noted.

			C1	C2	D1	D2	G1	G2
TYR	$\mu_{BP}^{app}$	mean $\pm$ sd	0.076 $\pm$ 0.025	0.066 $\pm$ 0.018	0.116 $\pm$ 0.008	0.194 $\pm$ 0.02	0.164 $\pm$ 0.019	0.1503 $\pm$ 0.003
		period	0 - 0.5	0 - 0.5	0 - 0.5	0 - 0.5	0 - 0.5	0 - 0.5
TYR	$\mu_{syn}^{app}$	mean $\pm$ sd	nd	nd	nd	nd	0.014 $\pm$ 0.05	0.033 $\pm$ 0.003
		Period					2 - 3	2 - 3
TYR	$\mu_{picoeuk}^{app}$	mean $\pm$ sd	nd	nd	nd	nd	0.024 $\pm$ 0.004	nd
		period					2 - 3	
ION	$\mu_{BP}^{app}$	mean $\pm$ sd	0.042 $\pm$ 0.007	0.041 $\pm$ 0.005	0.09 $\pm$ 0.02	0.14 $\pm$ 0.006	0.13 $\pm$ 0.01	0.14 $\pm$ 0.03
		Period	0 - 0.5	0 - 0.5	0 - 0.5	0 - 0.5	0 - 0.5	0 - 0.5
ION	$\mu_{syn}^{app}$	mean $\pm$ sd	nd	nd	0.011 $\pm$ 0.001	0.015 $\pm$ 0.001	0.038 $\pm$ 0.002	0.045 $\pm$ 0.008
		Period			0.5 - 2	0.5 - 2	0.5 - 2	0.5 - 2
ION	$\mu_{picoeuk}^{app}$	mean $\pm$ sd	0.018 $\pm$ 0.001	0.012 $\pm$ 0.007	0.043 $\pm$ 0.014	0.034 $\pm$ 0.014	0.057 $\pm$ 0.012	0.053 $\pm$ 0.008
		Period	0.5 - 3	0.5 - 2	0.5 - 2	0.5 - 2	0.5 - 2	0.5 - 2
FAST	$\mu_{BP}^{app}$	mean $\pm$ sd	0.020 $\pm$ 0.002	0.026 $\pm$ 0.003	0.089 $\pm$ 0.014	0.090 $\pm$ 0.007	0.12 $\pm$ 0.005	0.16 $\pm$ 0.014
		Period	0 - 0.5	0 - 0.5	0 - 0.5	0 - 0.5	0 - 0.5	0 - 0.5
FAST	$\mu_{syn}^{app}$	mean $\pm$ sd	0.022 $\pm$ 0.002	0.024 $\pm$ 0.002	0.039 $\pm$ 0.001	0.045 $\pm$ 0.003	0.064 $\pm$ 0.001	0.063 $\pm$ 0.001
		Period	0.5 - 2	0.5 - 2	0.5 - 2	0.5 - 2	0.5 - 2	0.5 - 2
FST	$\mu_{picoeuk}^{app}$	mean $\pm$ sd	0.020 $\pm$ 0.002	0.012 $\pm$ 0.001	0.023 $\pm$ 0.004	0.026 $\pm$ 0.001	0.040 $\pm$ 0.002	0.034 $\pm$ 0.005
		Period	0.5 - 2	0.5 - 2	0.5 - 2	0.5 - 2	0.5 - 2	0.5 - 2

872  
 873  
 874  
 875  
 876  
 877  
 878  
 879  
 880



881 **Figure legends:**

882 **Figure 1.** Bacterial and viral parameters in the three experiments (TYR, ION and FAST) in each minicosm  
883 (D1, D2, G1 and G2). The values are normalized to the controls: the data are presented as the difference  
884 between the treatments and the mean value of the duplicate controls. The first row represents the  
885 bacterial cell specific growth rates and relative mortality rates at t24h after dust addition. The second  
886 row represents the relative viral productions at t24h and at T0 for the G treatments. The last row  
887 represents the viral strategies: the percentages of lytic (FLIC) or lysogenic (FLC) cells at t24h and at T0 for  
888 the G treatments.

889 **Figure 2.** (A) Log-log linear regression between bacterial biomass and bacterial production, dotted lines  
890 represent linear regressions for each treatment. (B) Relationships between log HNF abundance and log  
891 bacterial prey abundance. Solid black and dotted black lines corresponds to the Mean Realized HNF  
892 Abundance (MRA) and theoretical Maximum Attainable HNF Abundance line (MAA) respectively. The  
893 samples are grouped per treatments.

894 **Figure 3.** Relative abundance of viral populations at the initial (*in situ*: at t-12h before dust addition) and  
895 final time points in all minicosms (C1, C2, D1, D2, G1 and G2) during the three experiments (TYR, ION  
896 and FAST).

897 **Figure 4.** nMDS plot of bacterial community composition over the course of the three experiments  
898 based on Bray-Curtis dissimilarities of 16S rDNA sequences. Samples clustering at different level of  
899 similarity are circled together. All circles represent clusters which are significantly different from each  
900 other ( $p < 0.05$ ) based on a PERMANOVA test.

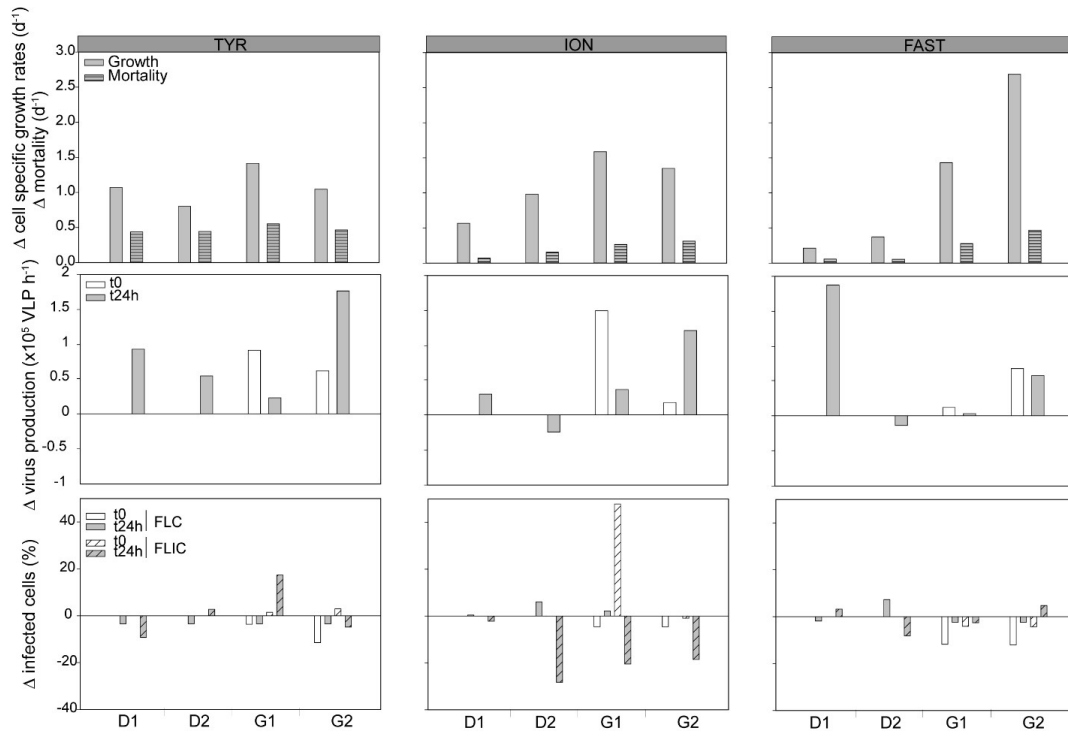
901 **Figure 5.** nMDS plot of micro-eukaryotes community composition over the course of the three  
902 experiments based on Bray-Curtis dissimilarities of 18S rDNA sequences. Samples clustering at different  
903 level of similarity are circled together. All circles represent clusters which are significantly different ( $p <$   
904  $0.05$ ) from each other based on a PERMANOVA test.

905

906

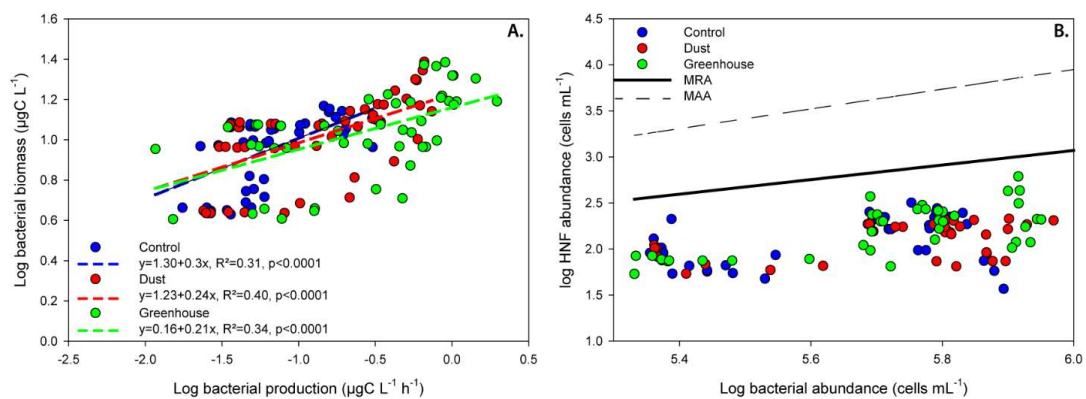


907



908

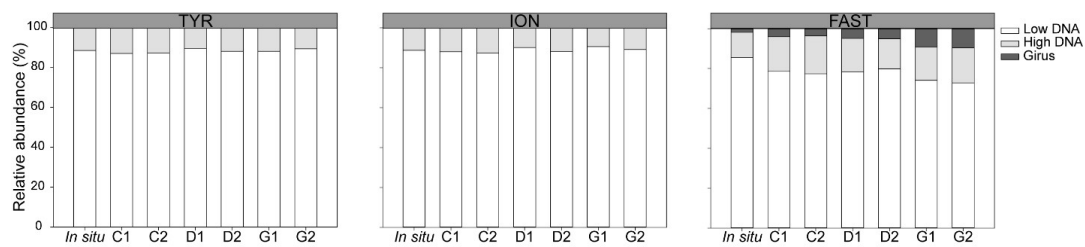
909 **Figure 1.**



910 **Figure 2.**

911

912



913

914 **Figure 3.**

915



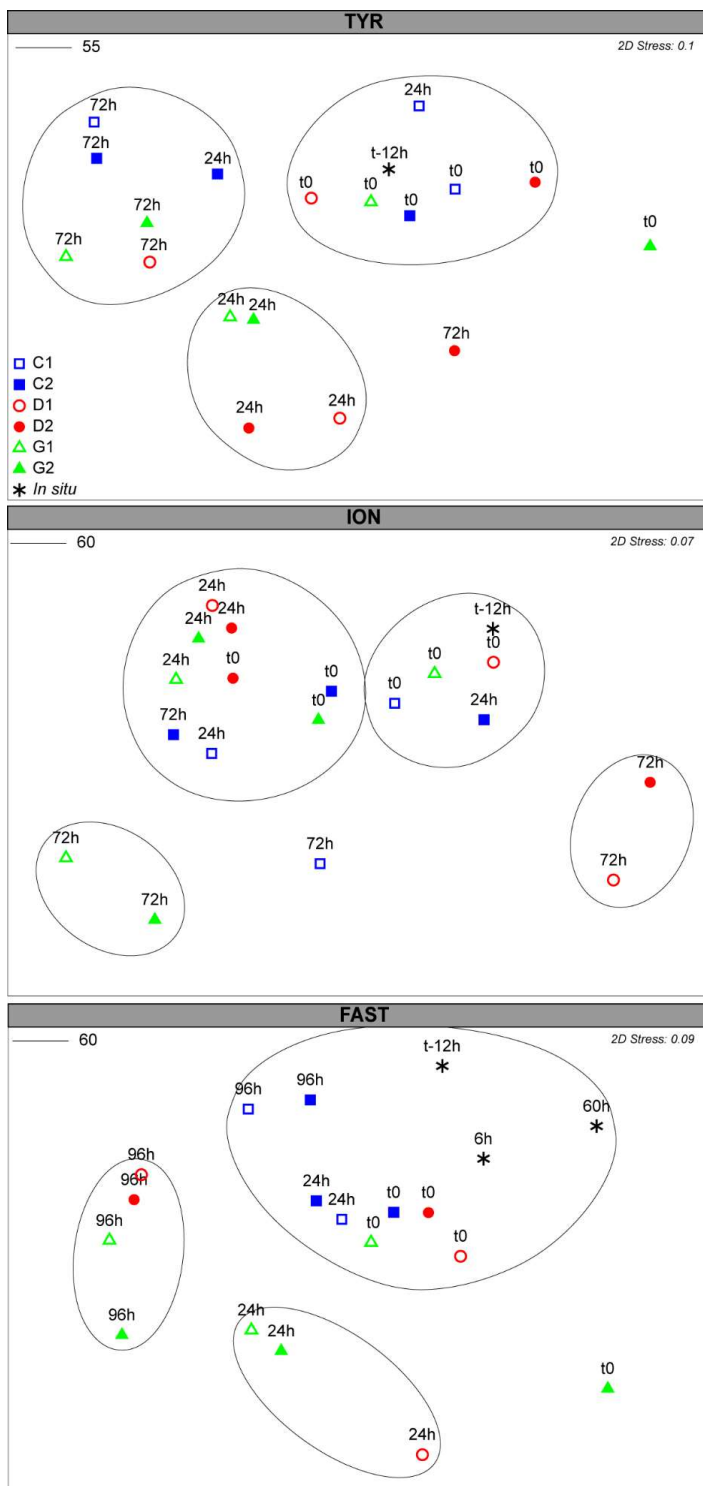


Figure 5.